JOURNAL OF SOLID STATE CHEMISTRY **138,** 66–73 (1998)
ARTICLE NO. SC987755

Charge Transfer–T_c Relation in the Superconducting Intercalates $IBi_2Sr_2CaCu_2O_y$

S.-J. Hwang, N.-G. Park, D.-H. Kim, and J.-H. Choy[1]

Department of Chemistry, Center for Molecular Catalysis, College of Natural Sciences, Seoul National University, Seoul 151-742, Korea

Received July 14, 1997; in revised form January 7, 1998; accepted January 8, 1998

Two different kinds of stage-1 iodine intercalates of $Bi_2Sr_2CaCu_2O_y$ with dissimilar T_c have been prepared in order to understand the relationship between superconducting properties and electronic structures. According to the XRD analysis and the magnetic susceptibility measurements, it is found that, in spite of the same basal increments for both intercalates ($\Delta d = \sim 3.6$ Å), the iodine intercalate prepared in a vacuum-sealed tube exhibits a larger T_c depression (13 K) compared to the iodine intercalate synthesized in air ($\Delta T_c = 6$ K). The origin of such different T_c shifts has been investigated by performing the systematic XANES/EXAFS analyses at the I L_1-, Cu K-, and Bi L_3-edges, where the charge transfer between host and guest is found to be strongly dependent on the reaction condition. From the BVS calculation based on the Cu K-edge EXAFS results, it is clarified that there is an excellent correlation between the amount of hole doping and T_c depression for both iodine intercalates. In this respect, we conclude that, regardless of lattice expansion along the *c*-axis, the T_c of Bi-based cuprate is wholly dependent on the hole concentration of the CuO_2 layer. © 1998 Academic Press

INTRODUCTION

The $Bi_2Sr_2CaCu_2O_y$ superconductor (Bi2212) has attracted much attention because of its anisotropic structural and transport properties, and has also been suggested as a good host matrix for the intercalation reaction due to a weak binding force between the BiO layers. This compound has an intergrowth structure in which the CuO_2 layers taking an active part in superconductivity are alternated with the other inactive ones along the *c*-axis. In this respect, one of the most interesting aspects of this superconductor is the question of how the superconducting property can be influenced by structural and electronic interactions between the layers. Although the copper valence (or hole concentration) is probably the most important variable responsible for the superconducting property of this material, the interblock electronic coupling between the next nearest CuO_2 layers via the Bi_2O_2 bilayers has also been considered to affect the superconductivity. It has been well known that the oxidation state of copper can be easily controlled by substituting some trivalent cations for the divalent Sr or Ca ones within the lattice. However, in this case, no information on the interlayer interaction between the CuO_2 layers is available because the basal spacing (*c*-axis parameter) remains unchanged after substitution. It is, therefore, thought that the intercalation reaction is one of the most powerful methods to investigate the superconducting property of the layered cuprates becauses it enables us to control simultaneously the copper valence and the crystal *c*-axis by charge transfer and lattice expansion, respectively.

Recently, we have developed new superconducting intercalation compounds, $(HgX_2)_{0.5}Bi_2Sr_2CaCu_2O_y$ (1, 2) and $(AgI)Bi_2Sr_2CaCu_2O_y$ (3, 4). Among them, we have found that the mercury salt intercalation into Bi2212 gives rise to a slight T_c depression of about 6–7 K even with the large lattice expansion along the *c*-axis ($\Delta d \approx 7.2$ Å). Compared to the previous results on the first-stage iodine intercalate (IBi2212) with $\Delta T_c \approx 10$ K and $\Delta d \approx 3.6$ Å (5), the interblock interaction was thought to be negligible for the mercury salt intercalates and their T_c was expected to be strongly related to the electronic structure of copper in the CuO_2 layers. This prediction was supported again by the recent report on the T_c evolution of La-substituted Bi2212 on $HgBr_2$ intercalation (6). On the other hand, it was previously claimed based on the susceptibility study of the stage 1 ($\Delta T_c \approx 10$ K) and stage 2 ($\Delta T_c \approx 5$ K) iodine intercalated samples that the interblock coupling effect may contribute to the T_c change (7); however, it is still ambiguous whether such a T_c depression for the latter is due to a half-reduction of interblock interactions or a half-hole doping per formula unit by the formation of $(I_{0.5})$Bi2212. To solve this problem, it is necessary to find intercalates with the same basal spacings, but with different copper valences by controlling the charge transfer rate. If such intercalates can be obtained, it is possible not only to investigate simultaneously the interblock coupling effect and charge transfer

[1] To whom correspondence should be addressed. Tel: (82)2-880-6658. Fax: (82)2-872-9864. E-mail: jhchoy@plaza.snu.ac.kr.

0022-4596/98 $25.00
Copyright © 1998 by Academic Press
All rights of reproduction in any form reserved.

effect, but also to understand which mainly contributes to the T_c depression.

According to the band calculation (8), it was found by an introduction of excess oxygen that the electronic structure of Bi2212 is very sensitive to the distortion of the Bi_2O_2 bilayer. Such a modification of a BiO layer gives rise to a significant change in the internal charge transfer between the CuO_2 and BiO layers, which is important for hole transfer from an intercalated iodine layer to a superconductive CuO_2 sheet. In this respect, we have attempted to prepare two iodine intercalates with different extents of hole doping by adopting different synthetic conditions. Their superconducting property–electronic structure relations have been carefully examined by performing X-ray absorption near edge structure (XANES) and extended X-ray absorption fine structure (EXAFS) analyses. In addition, on the basis of the Cu K-edge EXAFS fitting results, the bond valence sum (BVS) calculation has been carried out to determine an effective oxidation state of copper and to discuss the relationship between copper valence and T_c.

EXPERIMENTAL

Polycrystalline Bi2212 was prepared by conventional solid state reaction in an ambient atmosphere as previously described (9, 10), and its iodine intercalates were synthesized by adopting two different synthetic conditions. The first (denoted IA) was prepared by heating the mixture of Bi2212 and solid iodine at 190°C for 2 h in a tube, which was not completely sealed, but opened to air at one end with a capillary in order to keep the iodine vapor pressure, $P_1 \approx 1$ atm; the second (denoted IV) was prepared at 190°C for 2 h in a vacuum-sealed tube, $P_1 \approx 15$ atm. We have also carried out the same heat treatment for the pristine compound (denoted PT) as for the iodine intercalate prepared in air in order to check the T_c change induced by a possible oxygen uptake during the intercalation reaction.

The formations of the first-stage intercalate of $IBi_2Sr_2CaCu_2O_y$ under two different synthetic conditions were confirmed by both powder X-ray diffraction (XRD) and thermogravimetric (TGA) analyses.

To check superconducting properties of the samples, magnetic susceptibility was measured as a function of temperature by using a SQUID magnetometer in a field of 20 Oe the electrical resistance measurement was performed by the conventional four-probe method.

X-ray absorption experiments were carried out at the Photon Factory (National Laboratory for High Energy Physics, Tsukuba), operating at 2.5 GeV with a stored current of about 300–360 mA (11, 12). For measurement of the iodine L_1-edge absorption spectra, a Si (111) double crystal monochromator was detuned by 60% to minimize the effect of higher harmonics; a Si (311) channel-cut monochromator was used for measuring the Cu K- and Bi L_3-edge absorption spectra. The samples for X-ray absorption experiments were prepared in the form of a pellet, in which the finely ground samples were diluted with boron nitride in order to obtain an optimum absorption jump ($\Delta\mu t \approx 1$). The spectra were obtained in the transmission mode at room temperature, with gas ionization chambers as detectors.

All the XANES spectra presented here were normalized by fitting the smooth EXAFS high-energy region with a linear function after subtracting the background extrapolated from the pre-edge region. For the Cu K-edge EXAFS analysis, the EXAFS oscillations were separated from the absorption background by using a cubic spline background removal technique. The resulting $\chi(k)$ oscillations were weighted with k^3 in order to compensate for the diminishing amplitude of the EXAFS at high-k region. For analyzing the EXAFS data, a nonlinear least-squares curve fitting was carried out to the Fourier filtered first coordination shell by minimizing the value of F ($F = [\sum k^6(\chi_{cal} - \chi_{exp})^2]^{1/2}/n$, where the summation was performed over the data points n in the k range) with the use of well-known single scattering EXAFS theory (13).

RESULTS AND DISCUSSION

Figure 1 shows the powder XRD patterns for the pristine compound and its iodine intercalates. The lattice constants for the pristine ($a = 5.40$ Å and $c = 15.44$ Å) are not changed significantly after heat treatment at 190°C for 2 h under an ambient atmosphere ($a = 5.40$ Å and $c = 15.41$ Å). On iodine intercalation, the basal spacing is expanded by 3.73 Å for IA and 3.74 Å for IV, respectively, while the in-plane a parameter is not changed. It is worth mentioning here that the same extent of lattice expansion (the same stage-1 structure) was observed regardless of the synthetic conditions.

The temperature-dependent magnetic susceptibilities for the pristine compound and its iodine intercalates, IA and IV, are represented in Fig. 2. The superconducting transition temperature (T_c) was determined by extrapolating the linear part of the diamagnetic transition region. The pristine as-prepared and heat-treated (PT) samples show the same T_c of ~ 76 K, while the T_c for the iodine intercalates changes quite differently depending on the synthetic conditions. The T_c depression on intercalation (i.e., ΔT_c) is about 6 K for IA, significantly smaller than the value (13 K) for IV. Such results were also confirmed by electrical resistance measurements, where the T_c decreased induced by intercalation is found to be 7 K for IA and 12 K for IV. The above experimental finding allows us to conclude that the T_c evolution has no correlation with the lattice expansion, since both iodine intercalates have the same basal spacing. In this respect, it is expected that there are different degrees of charge transfer between host and guest for both intercalates, resulting in the dissimilar T_c shifts (14).

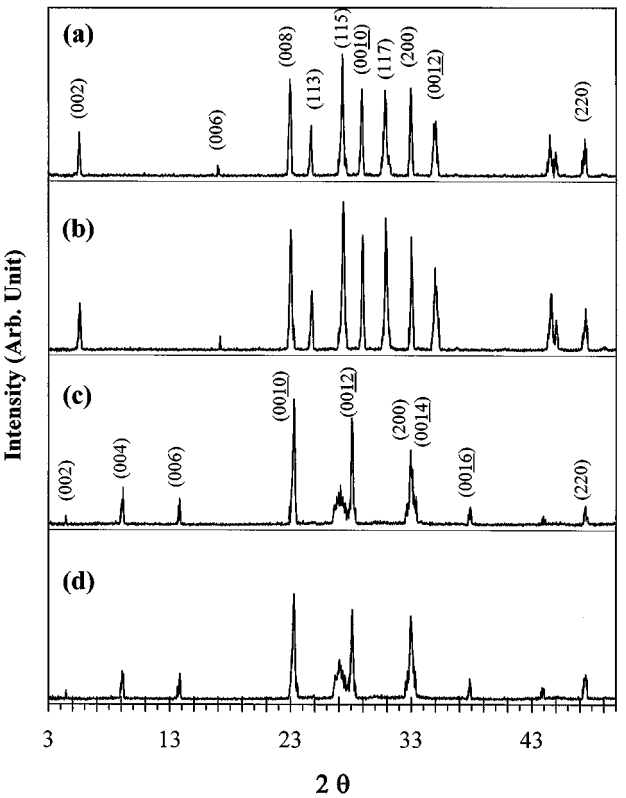

FIG. 1. Powder XRD patterns for (a) as-prepared Bi2212, (b) heat-treated Bi2212 at 190°C for 2 h under an ambient atmosphere, (c) IBi2212 prepared in a vacuum-sealed tube, and (d) IBi2212 prepared in a tube, but opened in air with a capillary ($P_I \approx 1$ atm). The as-prepared Bi2212 was used as host for the iodine intercalation.

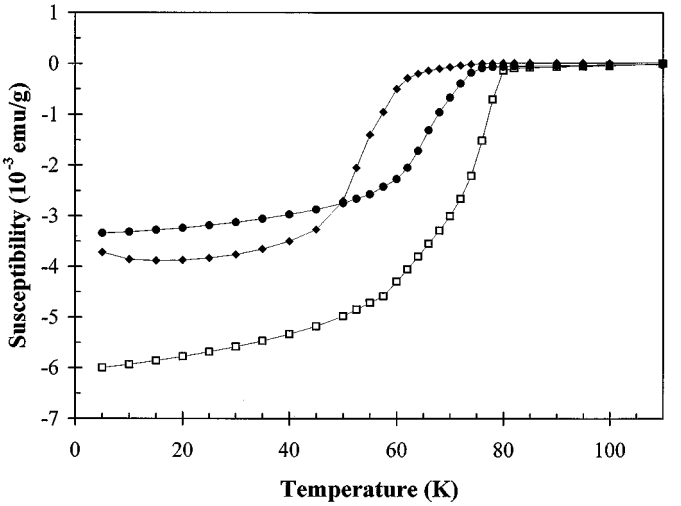

FIG. 2. Magnetic susceptibility vs temperature curves for Bi2212 (empty squares), IA (closed circles), and IV (diamonds), where the T_c was determined to be 76 K, 70 K, and 63 K, respectively. The intersection point of two straight lines was used to define the value of T_c. The susceptibility data for the Bi2212 sample after heat treatment have the same order as those for the as-prepared one.

In order to elucidate the electronic structure of the intercalated iodine species in IA and IV, XANES spectroscopic studies have been performed at the I L_1-edge. As shown in Fig. 3, the normalized I L_1-edge XANES spectra for the IBi2212 compounds with the reference iodine exhibit a characteristic single sharp peak around 5186 eV. This strong absorption resonance, called white line (WL), has been explained as the transition from 2*s* core level to unoccupied 5*p* states (15). Since the WL intensity is associated with the density of unoccupied final states (15–18), it can be used to estimate the number of available *p*-final states (i.e., the unoccupied *p*-hole count). It is worthy to note here that we have taken special care to exclude a possible error in determining the white-line intensity by measuring several spectra for each iodine-containing compound, varying the thickness of the sample, and we found that, at least in our experimental conditions, no change in white-line intensity was observed. In the spectrum of solid iodine, the WL peak is rather intense due to a fully unoccupied one-hole of the 5*p* orbital (i.e., $5p^5$ state). But this peak is not observed for KI because the iodine in KI exists in the form of I^- with fully occupied $5p^6$ states. It is also clearly found that the WL intensity for both iodine intercalates, IA and IV, is somewhat depressed compared to solid iodine, which indicates that the unoccupied 5*p* orbital is partially filled with the electron transferred from the host lattice. Moreover, the WL strength in IA is found to be less depressed with respect to

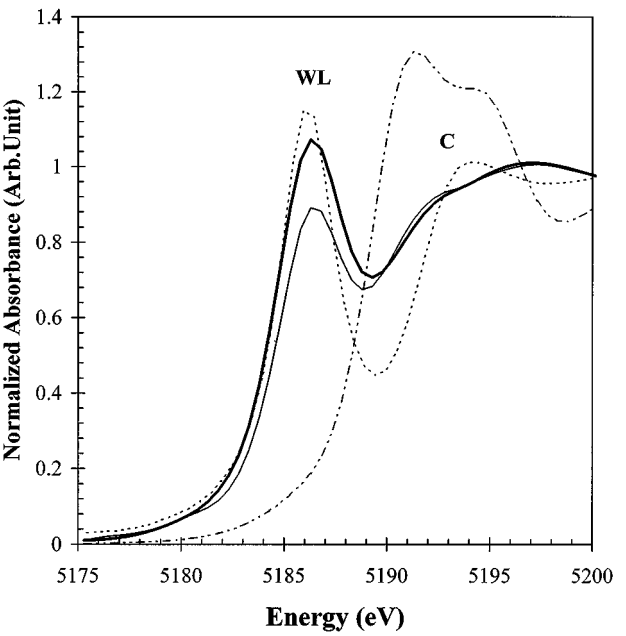

FIG. 3. Normalized I L_1-edge XANES spectra for IA (boldface solid lines) and IV (lightface solid lines), together with solid iodine (dashed lines) and KI (dot-dashed lines) as references.

IV. Taking into account the same iodine content for both intercalates, this underlines that the amount of transferred electron per iodine atom is smaller for the former than for the latter. The oxidation state of iodine could also be examined bassed on the variation of energy difference ($\Delta E = E_{WL} - E_C$) between the WL peak and the continuum peak (C) at about 5190 eV corresponding to the transition to the unbound continuum state. As shown in Fig. 3, there is a shift of the peak C to a lower-energy side for both iodine intercalates, resulting in a decrease of ΔE compared to the unintercalated iodine molecule. It is also observed that such a peak shift is less prominent for IA than for IV. According to the previous study on the iodine intercalated C_{60} (16), the energy difference between both peaks (ΔE), associated with the energy gap between the highest-occupied level and the unbound continuum state, is inversely proportional to the electron density of the antibonding state. Therefore, the observed change in ΔE on intercalation confirms that the vacant I 5p state of intercalated iodine is partially occupied by the electron from the host lattice and that the intercalated iodine in IA receives fewer electrons than in IV.

In order to get the quantitative information on charge transfer, the area of the pre-edge peak (A) has been calculated by employing a least-squares fitting program on the XANES data. Each spectrum is fitted with a superimposition of a Lorentzian line and an arctangent step line. In the curve-fitting procedure, the step value is fixed to unity and the others are allowed to vary. Least-squares fits of the absorption edge to the sum of the Lorentzian and step functions are shown in Fig. 4, where this simple two-component deconvolution gives a very satisfactory fit to the observed line shape. The parameters obtained from the best fit and the areas of the Lorentzian component for solid iodine, IA, and IV are listed in Table 1. It is obvious that the calculated area decreases systematically on going from solid iodine to IA and IV, as expected from this qualitative analysis. In Fig. 5, the WL area is plotted against the occupied p states along with the unoccupied p states, where the I 5p-orbital occupancy is assumed to be $5p^5$ and $5p^6$ for solid iodine and KI, respectively, in order to estimate the p-orbital occupancy of the intercalated iodine. The I

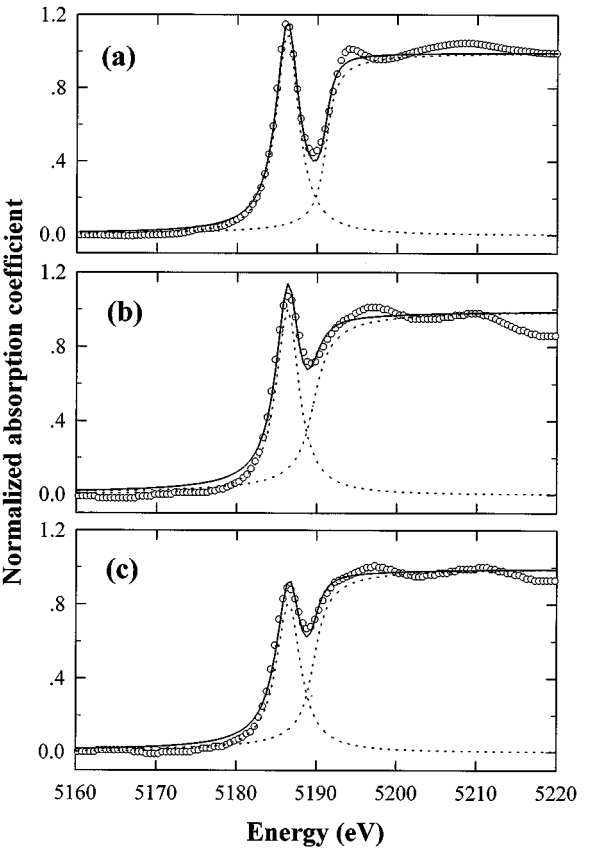

FIG. 4. Experimental I L_1-edge XANES data (open circles) and the fit to the sum of the Lorentzian and arctangent step functions (solid lines) for (a) solid iodine, (b) IV, and (c) IA. The separate components of this function are also shown by dotted lines.

TABLE 1
Lorentzian and Arctangent Curve Fitting Results of XANES Spectra for Solid Iodine, $IBi_2Sr_2CaCu_2O$ (IA), and $IBi_2Sr_2CaCu_2O_y$ (IV)

	Lorentzian line[a]			Arctangent line[b]			
Sample	f_{max}	σ_L(eV)	E_0 (eV)	T	σ_A (eV)	E_1 (eV)	White-line area[c]
Solid iodine	1.08	3.4	5186.2	1.0	1.9	5191.1	5.53
$IBi_2Sr_2CaCu_2O_y$ (IA)	1.00	3.5	5186.3	1.0	3.1	5189.6	5.08
$IBi_2Sr_2CaCu_2O_y$ (IV)	0.80	3.7	5186.5	1.0	2.6	5189.7	4.32

[a] Symbols f_{max}, σ_L, and E_0 represent the maximum amplitude, full-width-half-maximum, and energy at f_{max} of the Lorentzian line, obtained by fitting the following Lorentzian equation to the normalized XANES data: $f(E) = f_{max} \times [(\sigma_L/2)^2/((\sigma_L/2)^2 + (E - E_0)^2)]$, where f_{max} is $[a/(\pi \times (\sigma_L/2))]$ (a is constant).

[b] Symbols T, σ_A, and E_1 represent the step, full-width-half-maximum, and inflection energy of the arctangent line, obtained by fitting the following arctangent step function to the normalized XANES data: $f(E) = T \times [(1/\pi) \times \arctan((E - E_1)/(\sigma_A/2)) + 1/2]$.

[c] The white-line area is obtained by integrating the Lorentzian line.

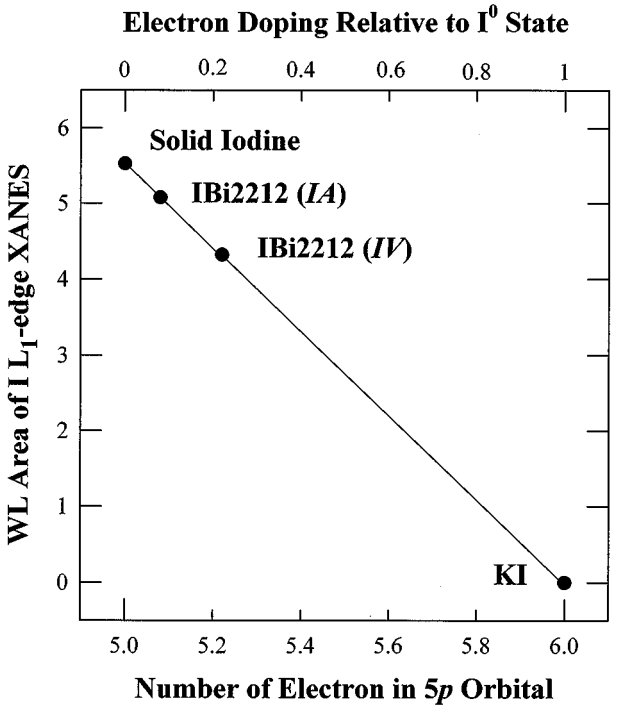

FIG. 5. Relationship between the WL area and the electron occupancy in 5*p* states for the iodine intercalates, IA and IV, together with the reference compounds solid iodine ($5p^5$) and KI ($5p^6$). The amount of electrons transferred to the intercalated iodine is also represented relative to the value of solid iodine as zero.

5 *p*-orbital occupancy for IA and IV is deduced approximately from the plot and found to be $5p^{5.08}$ and $5p^{5.22}$, which clarifies the degree of electron transfer to iodine from the host lattice depending on the intercalation reaction conditions. Therefore, it is expected that the oxidation state of the CuO_2 layer also changes differently for both iodine intercalates, IA and IV, on intercalation.

Figures 6a and 6b represent the Cu *K*-edge XANES spline and second derivative spectra for the pristine Bi2212 and its iodine intercalates, IA and IV, respectively. As shown in the figure, there is on intercalation an overall spectral shift toward a high-energy side of 0.1 eV for IA and 0.2 eV for IV, indicating oxidation of the CuO_2 layer, in good agreement with the present I L_1-edge XANES results. In order to get detailed information on the electronic and geometric structures of the copper–oxygen layer, each spectrum has been carefully investigated using the second differential method, which is quite effective in differentiating a small difference of spectral features. A small pre-edge peak (denoted *P*) is observed for all the present compounds; it is explained as the quadrupole-allowed transition from the core 1*s* level to the unoccupied 3d state. The energy of this peak is found to be slightly higher for both intercalates than for the pristine compound, coinciding with the shift of edge position. In the main edge region, there are some peaks corresponding to the dipole-allowed transitions from the core 1*s* level to the unoccupied 4*p* states, which are denoted A, A′, B, and C. According to our previous Cu K-edge XAS study (19), the main edge features A and B are attributed to the transition from the 1*s* orbital to the out-of-plane $4p_\pi$ orbital, with and without shakedown processes, whereas the features A′ and C are ascribed to the in-plane $4p_\sigma$ orbital transition with and without shakedown processes (20, 21). As can be seen clearly from Fig. 6b, all the main edge peaks move toward the high-energy side on intercalation, suggesting the destabilization of antibonding Cu 4p final states, which are closely related with a change in the local structure of the CuO_2 plane.

Such a structural modification could be checked out directly by performing Cu *K*-edge EXAFS analysis. Figure 7

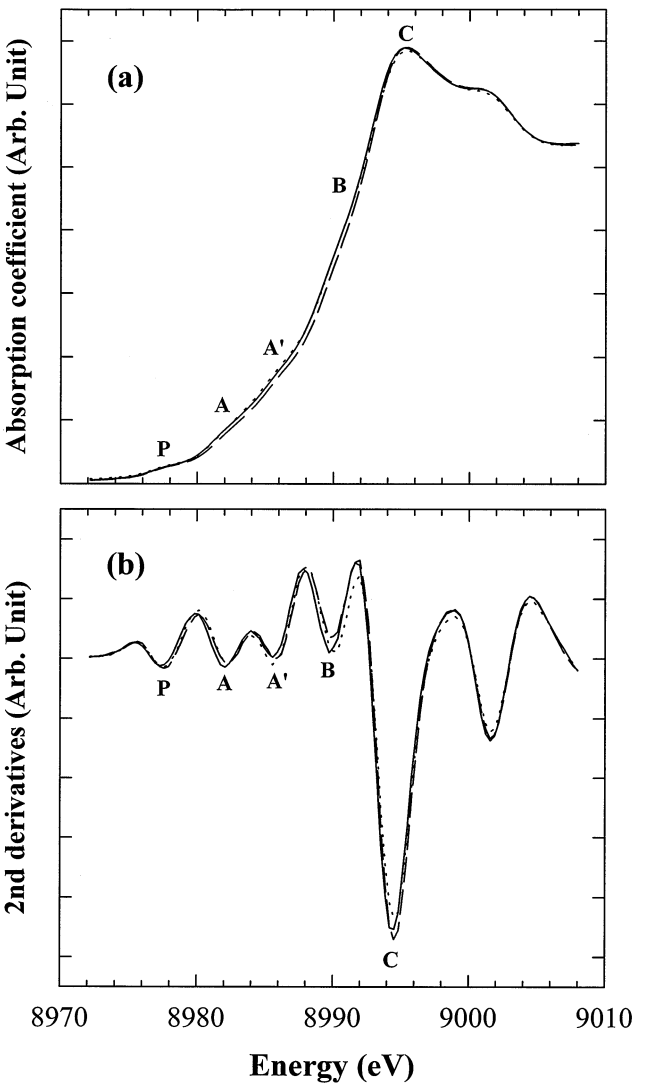

FIG. 6. Cu K-edge XANES (a) spline and (b) second derivative spectra for Bi2212 (solid line), IA (dotted lines), and IV (dashed line).

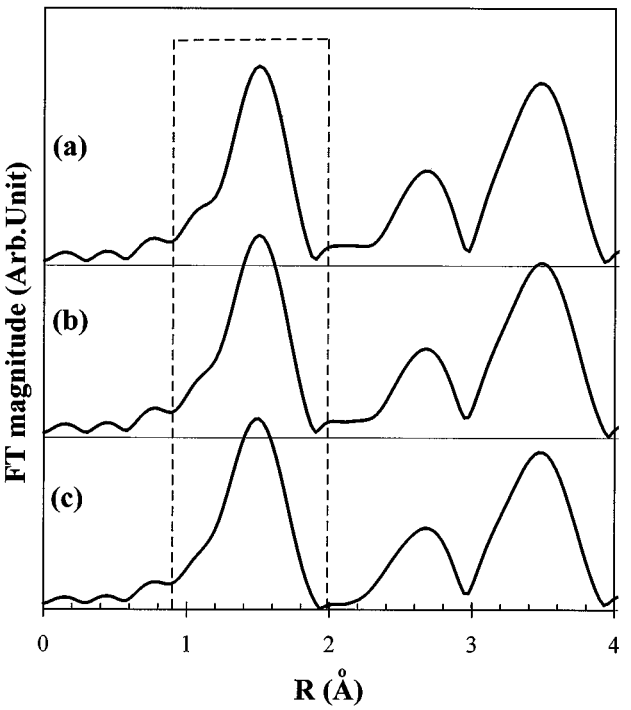

FIG. 7. Fourier transforms of k^3-weighted Cu K-edge EXAFS for (a) Bi2212, (b) IA, and (c) IV, along with the filtering windows (dashed lines). The first peak in each spectrum corresponds to the (Cu–O) shell.

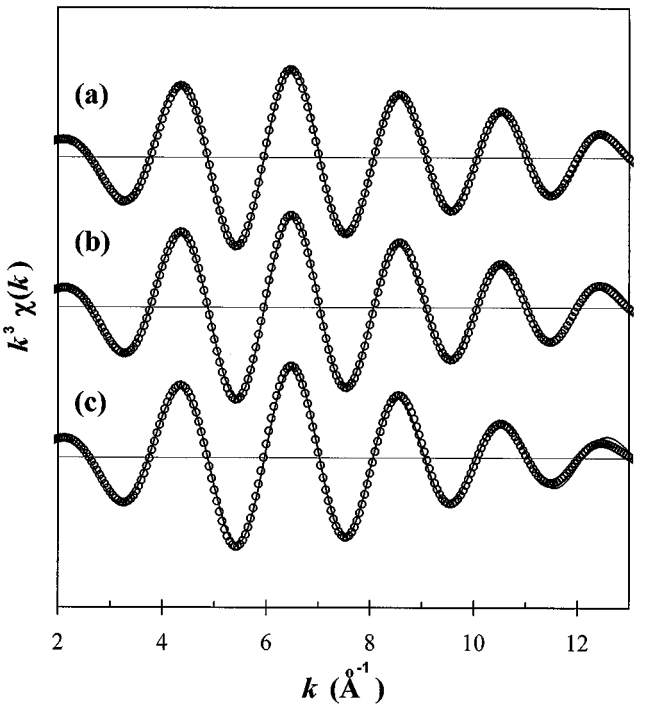

FIG. 8. Fourier-filtered experimental EXAFS of the first peak (open circles) and the least-squares best fit (solid lines) for (a) Bi2212, (b) IA, and (c) IV.

shows the Fourier transforms (FT) of the Cu K-edge EXAFS spectra. The first peak in the FT corresponds to the nearest neighbors of the copper ion, i.e., a (Cu–O) shell. This peak was inverse Fourier-transformed into the k space (Fig. 8) for the curve-fitting analysis. In the fitting procedure, only the distance (R) and the Debye-Waller factor (σ^2) were allowed to be refined; the coordination number (N) was fixed to a crystallographic value because of the inaccuracies in refining the N values caused by strong correlation with σ^2. The best fitting results to the first coordination shell are compared with the experimental spectra in Fig. 8 and the fitted structural parameters are listed in Table 2. It is found from the present EXAFS analysis that the intercalation has little effect on in-plane (Cu–O) bond distances, while out-of-plane (Cu–O) bond distances are slightly shortened on intercalation. Such a result is not surprising, since the intercalation influences the crystal parameter c by increasing the basal spacing, but does not affect the a parameter as in the XRD analysis.

Using the (Cu–O) bond distance obtained from the EXAFS analysis, the oxidation state of Cu in CuO_5 pyramid could be estimated on the basis of the BVS method. The BVS, which represents the effective valence or the oxidation state of an atom, is defined (22) as

$$V(i) = \sum_j \exp[(R_0 - R_{ij})/0.37], \qquad [1]$$

where $V(i)$ is the bond valence sum of the ith atom, R_{ij} is the distance between the ith and jth atoms, and R_0 is an empirical parameter dependent on the atomic species and their valence states. Since R_0 depends on the oxidation state, it should give a different value for the (Cu–O) bond as the oxidation state of copper varies (23). For example, R_0 has a value of 1.600 Å for Cu^{1+}, 1.679 Å for Cu^{2+}, and 1.739 Å for Cu^{3+}. Therefore, there is a problem in using R_0 to calculate the BVS of copper in the given compounds. Brown (24) has pointed out that if the BVS calculated by assuming the oxidation state to be 2+ (labeled V'') exceeds 2, one can calculate it by assuming the oxidation state to be 3+ (labeled V'''). This procedure produces the correct oxidation state (V) as given by the following equation:

$$V(\mathrm{Cu}) = 2 + (V'' - 2)/(V'' + 1 - V'''). \qquad [2]$$

Since the oxidation state of copper in the p-type superconductors has a formal valence between 2 and 3 (25), the BVS for the pristine comound and its iodine intercalates, included among p-type superconductors, is calculated based on Eq. [2]. In Table 2, it is found that the calculated BVS of copper increases on going from the pristine compound to IA and IV, and increases with decreasing T_c, which is consistent with the tendency for the intercalated iodine in IA to be

TABLE 2

Bond Distance R_{ij}, Debye-Waller Factor σ_{ij}^2, and Bond Valence Sum (BVS) for $Bi_2Sr_2CaCu_2O_y$, $IBi_2Sr_2CaCu_2O_y$ (IA), and $IBi_2Sr_2CaCu_2O_y$ (IV)

Compound	Bond	R_{ij} (Å)[a]	σ_{ij}^2 ($\times 10^{-3}$ Å)[a]	No. of Bonds	BVS V''	BVS V'''
$Bi_2Sr_2CaCu_2O_y$	$Cu–O_{eq}$	1.903	3.257	4	2.180	2.504
($T_c = 76$ K)	$Cu–O_{ax}$	2.367	4.639	1	0.156	0.179
					2.336	2.683
					2.514	
$IBi_2Sr_2CaCu_2O_y$ (IA)	$Cu–O_{eq}$	1.903	3.794	4	2.180	2.504
($T_c = 70$ K)	$Cu–O_{ax}$	2.358	5.371	1	0.160	0.183
					2.340	2.687
					2.521	
$IBi_2Sr_2CaCu_2O_y$ (IV)	$Cu–O_{eq}$	1.898	5.102	4	2.212	2.540
($T_c = 63$ K)	$Cu–O_{ax}$	2.347	7.688	1	0.164	0.189
					2.379	2.729
					2.581	

[a] The bond distances and Debye-Waller factors of (Cu–O) are obtained by fitting the EXAFS data.

[b] The corrected BVS (V) of Cu is calculated by the relation

$$V(\mathrm{Cu}) = 2 + (V'' - 2)/(V'' - 1 + V'''),$$

where V'' and V''' are the BVSs calculated by assuming the oxidation state to be 2+ and 3+, respectively.

more doped with electrons than that in IV (from the previous I L_1-edge XANES results).

Such a dependence of hole doping on synthetic conditions can be understood as a result of the evolution of electronic structure. According to band calculations (26, 27), X-ray absorption spectroscopic studies (28), and photoemission experiments (29, 30), it has been suggested that the Bi 6*p* band intersects E_F and, therefore, accepts an electron from the Cu 3*d* band, resulting in a self-doping of hole into the CuO_2 layer. Even though the other band calculation based on the modulated structure of the Bi_2O_2 layer predicted that the bottom of the Bi 6*p* band lies more than 1 eV above the Fermi level (8), the oxidation of the CuO_2 layer on intercalation due to the hole donation from the intercalated iodine between Bi_2O_2 bilayer, shows that the internal redox mechanism is working in the present iodine intercalates (31). In this respect, the different oxidation states of iodine and copper for IA and IV should be attributed to the evolution of Bi 6*p* band energy induced by excess oxygen introduced during the intercalation reaction in air. Although the pristine compound annealed at 190°C in air (PT) is found to show negligible change in T_c compared to the intercalates, a small oxygen loading might give rise to an increase of Bi 6*p* band energy through the structural distortion of Bi_2O_2 bilayer (8). This would prevent an effective charge transfer between CuO_2 and BiO layers, giving rise to a smaller hole doping for IA, compared to IV. In fact, such an increase of oxygen content during the intercalation reaction in air is indirectly shown by the fact that the *c*-axis parameter of the pristine compound as prepared ($c = 15.44$ Å), which is inversely proportional to oxygen content (32), is found to be slightly shortened after heat treatment at 190°C for 2 h in air ($c = 15.41$ Å).

Figure 9 represents the Bi L_3-edge XANES spectra for the pristine compound and its iodine intercalates. There are three broad peaks, indicated as A, B, and C, in all the present spectra. Among them, the pre-edge peak *A* is attributed to the $2p_{3/2} \rightarrow 6s$ transition, while the main-edge peaks *B* and *C* in the high-energy side are attributed to the $2p_{3/2} \rightarrow 6d_{t_{2g}}$ and $2p_{3/2} \rightarrow 6d_{e_g}$ transitions, respectively (28). Based on the above assignments, the effect of intercalation on the Bi_2O_2 bilayer has been precisely investigated by

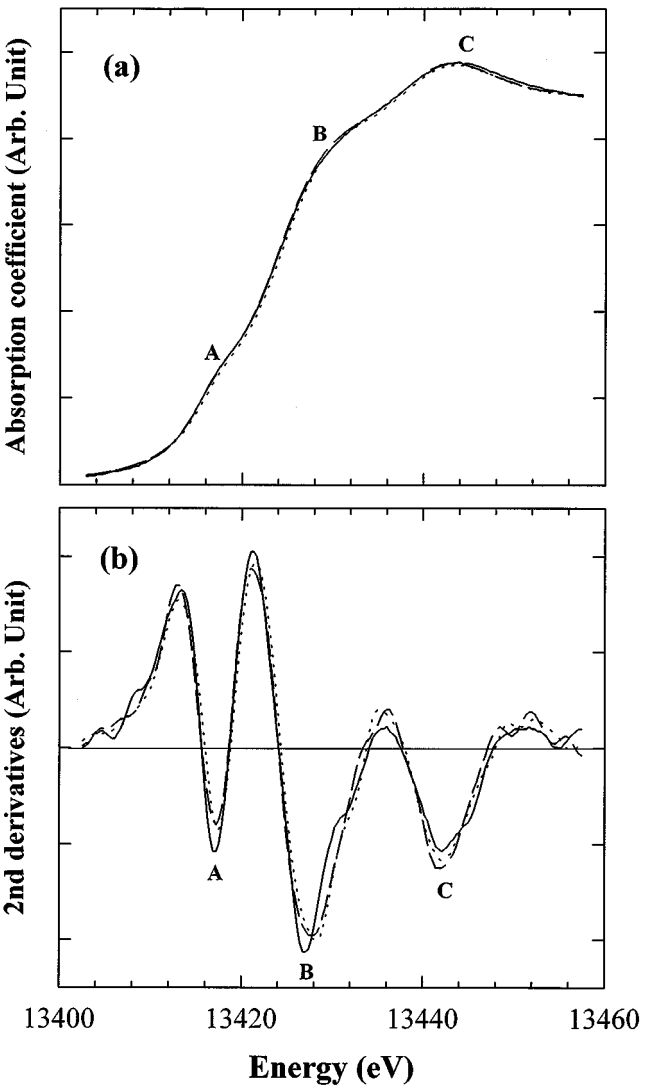

FIG. 9. Bi L_3-edge XANES (a) spline and (b) second derivative spectra for Bi2212 (solid line), IA (dotted lines), and IV (dashed line).

examining the second derivatives of the pristine compound and its iodine intercalates. As shown in Fig. 9b, the edge energy is significantly increased on intercalation for IA, in contrast to IV, indicating that the oxidation state of Bi is higher for the former. Such a result provides a clear evidence of the above speculation that the higher energy of the Bi 6*p* band for IA than for IV is responsible for a smaller charge transfer between iodine and the CuO_2 layer in the former. In addition to the shift of edge position, the intercalation of iodine gives rise to a decrease in the energy different between the peaks *B* and *C*. Even though this energy difference is not exactly equal to the ground state crystal field parameter ($10Dq$), the peak splitting is surely proportional to the strength of the crystal field. Therefore, the observed decrease in energy difference reflects the weakening of the crystal field around Bi on intercalation. This is surely attributed to an increase of the ($Bi–O_{Sr}$) bond distance as found from the Cu K-edge EXAFS results. The apical oxygen is coordinated with a copper ion in one direction and, at the same time, a bismuth ion in the other (33), and therefore it is expected that a remarkable shortening of the ($Cu–O_{Sr}$) bond induces an increase of the competing ($Bi–O_{Sr}$) bond distance, leading to a weakening of the crystal field around Bi.

Summarizing the present XANES/EXAFS results together with the BVS calculation, it is concluded that the intercalation of iodine enhances the average oxidation state of the CuO_2 layer through the electron transfer from host lattice to guest iodine, which is surely an origin of T_c evolution on intercalation. It is also clarified that the oxygen content of the pristine sample has a significant influence on the internal charge transfer between the BiO and CuO_2 layers.

ACKNOWLEDGMENTS

This work was supported in part by the Ministry of Education (BSRI-97-3413). The Research Institute of Molecular Science assisted in meeting the publication cost of this article.

REFERENCES

1. J.-H. Cloy, N.-G. Park, S.-J. Hwang, D.-H. Kim, and N. H. Hur, *J. Am. Chem. Soc.* **116,** 11564 (1994).
2. J.-H. Choy, S.-J. Hwang, and N.-G. Park, *J. Am. Chem. Soc.* **119,** 1624 (1997).
3. J.-H. Choy, N.-G. Park, Y.-I. Kim, S.-H. Hwang, J.-S. Lee, and H.-I. Yoo, *J. Phys. Chem.* **99,** 7845 (1995).
4. J.-H. Choy, N.-G. Park, S.-J. Hwang, and Y.-I. Kim, *Synth. Met.* **71,** 1551 (1995).
5. X.-D. Xiang, S. McKernan, W. A. Vareka, A. Zettl, J. L. Corkill, T. W. Barbee III, and M. L. Cohen, *Nature* **332,** 145 (1990).
6. J.-H. Choy, N.-G. Park, S.-J. Hwang, and Z. G. Khim, *J. Phys. Chem.* **100,** 3783 (1996).
7. X.-D. Xiang, W.A. Vareka, A. Zettl, J. L. Corkill, T. W. Barbee III, M. L. Cohen, N. Kijima, and R. Gronsky, *Science* **254,** 1487 (1991).
8. J. Ren, D. Jung, M. H. Whangbo, J. M. Tarascon, Y. Le Page, W. R. Mckinnon, and C. C. Torardi, *Physica C* **158,** 501 (1989).
9. J. M. Tarascon, W. R. McKinnon, P. Barboux, D. M. Hwang, B. G. Bagley, L. H. Greene, G. W. Hull, Y. Lepage, N. Stoffel, and M. Giroud, *Phys. Rev. B* **38,** 8885 (1988).
10. J.-H. Choy, S.-J. Kim, J.-C. Park, F. K. Frohlich, P. Dordor, and J. C. Grenier, *Bull. Korean Chem. Soc.* **11,** 654 (1990).
11. H. Oyanagi, T. Matsushida, M. Ito, and H. Kuroda, *KEK Report* **83,** 30 (1984).
12. H. Kuroda and A. Koyama, *KEK Report* **84,** 19 (1989).
13. B. K. Teo, "EXAFS: Basic Principles and Data Analysis." Springer-Verlag, Berlin, 1986.
14. Since no T_c shift was observed for the pristine compound before and after heat treatment at 190°C for 2 h under an ambient atmosphere, we can rule out the possibility that such different T_c decreases for both intercalates originate from the introduction of oxygen during intercalation reaction.
15. J.-H. Choy, D.-K. Kim, S.-G. Kang, D.-H. Kim, and S.-J. Hwang, "Superconducting Materials," (J. Etourneau, J. B. Torrance, and H. Yamauchi, Eds.), IITT-International, Paris, p. 329. 1993.
16. N.-G. Park, S.-W. Cho, S.-J. Kim, and J.-H. Choy, *Chem. Mater.* **8,** 324 (1996).
17. J. A. Horsley, *J. Chem. Phys.* **76,** 1451 (1982).
18. D. H. Pearson, C. C. Ahn, and B. Fultz, *Phys. Rev. B* **47,** 8471 (1993).
19. J.-H. Choy, D.-K. Kim, S.-H. Hwang, and G. Demazeu, *Phys. Rev. B* **50,** 16631 (1994).
20. R. A. Bair and W. A. Goddard III, *Phys. Rev. B* **22,** 2767 (1980).
21. N. Kosugi, H. Kondoh, H. Tajima, and H. Kuroda, *Chem. Phys.* **135,** 149 (1989).
22. I. D. Brown and D. Altermatt, *Acta Crystallogr. Sect. B* **41,** 244 (1985).
23. I. D. Brown, *J. Solid State Chem.* **82,** 122 (1989).
24. I. D. Brown, *J. Solid State Chem.* **90,** 155 (1989).
25. R. J. Cava, *Science* **247,** 656 (1990).
26. L.-F. Mattheiss and D.-R. Hamann, *Phys. Rev. B* **38,** 5012 (1988).
27. W.-E. Pickett, *Rev. Mod. Phys.* **61,** 433 (1989).
28. R. Retoux, F. Studer, C. Michael, B. Raveau, A. Fontaine, and E. Dartyge, *Phys. Rev. B* **41,** 193 (1990).
29. R. Böttner, N. Schroeder, E. Dietz, V. Gerhardt, W. Assmers, and J. Kowalewski, *Phys. Rev. B* **41,** 8679 (1990).
30. F. V. Hillebrecht, J. Fraxadas, L. C. Bourne, P. Pinsukayama, and A. Zettl, *Phys. Rev. B* **39,** 236 (1989).
31. This might be related to the structural modification of the (Bi–O) layer induced by introducing the foreign molecule into the interlayer space, which gives rise to the intersection of the Bi 6*p* band with E_F.
32. Y. Deshimaru, T. Otani, Y. Shimizu, N. Miura, and N. Yamazoe, *Jpn. J. Appl. Phys.* **30,** L1798 (1991).
33. K. Yvon and M. Francois, *Z. Phys. B* **76,** 413 (1989).